C.2a.1.11-Adsorption behavior of Cr (VI) from aqueous.pdf

By Risfidian Mohadi

WORD COUNT	4045	TIME SUBMITTED	22-JAN-2022 10:44AM
		PAPER ID	81672873

Adsorption behavior of Cr (VI) from aqueous solution by Fe-pillared acid activated Indonesian bentonite

Cite as: AIP Conference Proceedings **2194**, 020124 (2019); https://doi.org/10.1063/1.5139856

Tarmizi Taher, Neza Rahayu Palapa, Risfidian Mohadi, et al.

Adsorption Behavior of Cr (VI) From Aqueous Solution by Fe-Pillared Acid Activated Indonesian Bentonite

Tarmizi Taher[1], Neza Rahayu Palapa[2], and Risfidian Mohadi[2], Aldes Lesbani[1,a)]

[1]*Department of Environmental Sciences, Graduate School of Sriwijaya University, Jl. Padang Selasa, No. 524, Bukit Besar, Palembang, Indonesia*
[2]*Department of Chemistry, Faculty of Mathematics and Natural Sciences, Sriwijaya University, Jl. Palembang-Prabumulih, Km 32, Ogan Ilir, South Sumatra, Indonesia*

[a)] *Corresponding author: aldeslesbani@pps.unsri.ac.id*

Abstract. Hexavalent chromium is one of the most toxic pollutants released in the environment by various human activities. In this work, the removal of Cr (VI) from aqueous solution has been investigated using modified natural bentonite as the low-cost based material. Natural bentonite has been modified by two-step modifications, acid activation followed by iron pillarization. The bentonite products, before and after the modification have been characterized using X-ray diffraction and FT-IR in order to investigate the change of the bentonite properties. The further study of Cr (VI) adsorption on modified bentonite was explored by conducting a batch adsorption experiment in various operational parameter including adsorbent dosage, initial pH, contact time, initial Cr (VI) concentration, and temperature. The studied on the kinetics adsorption revealed that the Cr (VI) adsorption follows the pseudo-second-order model rather than the pseudo-first-order model. The investigation about the adsorption equilibrium at various initial Cr (VI) concentration apparently informed that the adsorption isotherm model is better interpreted with Langmuir model rather than Freundlich. The thermodynamic study on the Cr (VI) adsorption revealed that the adsorption process has endothermic behaviour and occurred spontaneously.

INTRODUCTION

Contamination of toxic heavy metal in wastewater from industrial effluent is one of the most significant factors causing the environmental issues worldwide. The presence of heavy metal in the environment, particularly in an aquatic environment, leads to the organism mortality due to its high toxicity and its capability to be accumulated in a living organism and dispersed through the food chain system [1]. Chromium is one of the most widely utilized heavy metals in human livelihood. It has been utilized in various industries, i.e., manufacture, tanning, leather, photography, glass, craft, and electroplating due to its unique characteristic. In other hands, chromium is also one of the most notorious heavy metals. Although chromium has many chemical valence states (-4 to +6), chromium in the hexavalent state (Cr (VI)) is the most toxic. Compared with the Cr III, which is the most abundant chromium state, Cr (VI) has almost 100-fold in toxicity properties [2]. As reported by Kumar et al. [3], Cr (VI) leads to various diseases including lung cancer, kidney circulation, dermatitis and even causing mortality. Consequently, the removal of Cr (VI) contamination in wastewater before discharge into the water body is mandatory in order to maintain the aquatic ecosystem and to conserve the freshwater resource.

For the last decades, various wastewater treatment methods to reduce and remove heavy metal contamination have been widely investigated. Bio-reduction/bioremediation [4], photocatalytic [5], ion exchange [6], ultra-filtration [7], chemical filtration [8], electrochemical process [9], and adsorption [3,10] have been intensively tested and utilized for Cr (VI) removal both in the laboratory and industrial scale. However, adsorption is the most intensive method studied based on previously published papers [2,11–14]. Adsorption is a well-known separation technique applied in the removal of a hazardous substance with higher effectivity compared by the other's technique.

In the industrial scale, the application of the adsorption process in the effluent treatment is limited by its high-cost operation, particularly the high-cost of the adsorbent production. In order to overcome this limitation, nowadays

The 2nd International Conference on Science, Mathematics, Environment, and Education
AIP Conf. Proc. 2194, 020124-1–020124-9; https://doi.org/10.1063/1.5139856
Published by AIP Publishing. 978-0-7354-1945-2/$30.00

various inexpensive and abundant materials have been employed and developed as an alternative adsorbent to remove heavy metal contamination in wastewater. Lignocellulosic based material [15], natural peat [16], termite nest [17], and clayey based material [18,19], as a low-cost natural abundant material have been investigated to be potential adsorbent material for Cr (VI) removal.

Recently, clays and clay minerals utilization as an adsorbent gained high concern due to its high surface area and high ion exchange capability. Bentonite is one of the most studied clays over the other clays such as kaolin, ball clay, laponite, and fuller's earth. Bentonite is mainly composed of montmorillonite minerals, a 2:1 (tetrahedral: octahedral) type of aluminosilicate layer. Naturally, the surface of bentonite clay has net negative charges that balanced by the exchangeable inorganic cation located in the interlamellar space such as Ca^+, Na^+ and H^+ [20]. This chemical nature allows the modification of bentonite structure by replacing the exchangeable cation with the other cation with better properties such as aluminum polyoxy, and hydroxy-iron to elevate its surface properties [21,22].

In our present study, a novel adsorbent material for Cr (VI) removal has been prepared by acid activating bentonite followed by Fe-pillaring using $FeNO_3$ precursor. The change of the bentonite properties due to the acid activation and pillarization process was characterized by XRD and FT-IR. The adsorption behavior of Cr (VI) on the modified bentonite sample was investigated by batch adsorption technique.

EXPERIMENTAL SECTION

Materials

Raw bentonite samples used in this work were collected from bentonite deposit located in Sarolangun District of Jambi Province, Indonesia. Prior further modification, the raw bentonite sample was soaked with distilled water for one night then rinsed several times to remove the impurities and it was dried in a hot air oven. The fine powder of bentonite samples was produced by milling in a grinder followed by sieving pass through a 200-mesh ASTM standard sieve. The powdered bentonite samples were labeled as NB.

The chemicals employed in this work, including sodium carbonate, iron nitrate, potassium dichromate, and sodium hydroxide were purchased from Merck Millipore, Singapore. Hydrochloric acid solution and 1,5-diphenylcarbazide were obtained from Sigma Aldrich. All the chemical used in this work were A.R. grade and used as received without further purification.

Preparation of acid activated bentonite

An acid activation was subjected to the bentonite sample in order to increase its properties and slightly change the bentonite crystallinity. The acid activation was carried out according to the previously reported paper by Faghihian and Mohammadi (2013). In brief, 127 mL of H_2SO_4 2 M was contacted with 30 g of bentonite sample and stirred for two hours at 60 °C in a beaker flask. After finished, the slurry was produced and cooled to room temperature. The slurry then separated by centrifugation and washed with distilled water for several times until pH was 6 to remove the access to the SO_4^{2-} ion. The acid activated bentonite product then dried, grinded and stored in a closed flask and labeled as H-B.

Preparation Fe pillaring solution

The pillaring solution was prepared based on the previous paper reported by Cao et al., (2013) with slight modification. Na_2CO_3 solution and iron nitrate solution were firstly prepared in the separated flask. Na_2CO_3 solution (0.5 mol L^{-1}), as much as 100 mL, was added drop wisely into a rounded-bottom flask containing 250 mL of iron nitrate 0.2 mol L^{-1} under vigorous stirring. The solution then continuously stirred for 24 h at room temperature. After finished, the solution then aged at room temperature for two days to obtain the pillaring agents.

Preparation Fe-pillared acid activated bentonite

Fe-pillared acid activated bentonite was prepared by dispersing 20 g of bentonite into 200 mL of deionized water. The prepared pillaring agent then added into prepared bentonite suspension. The mixture then stirred for two h under vigorous stirring and after finished aged at 100 °C for two days. The bentonite mixture then separated by centrifugation, washed several times with distilled water, and then dried at 80 °C for 24 h. The obtained solid bentonite then grinded to pass through 100 mesh standard sieve then calcined at 400 °C for three hours. The pillared bentonite product then stored in closed bottle flask named as H-FePilB.

Materials Characterization

X-ray diffraction (XRD) analysis was subjected to the natural bentonite and modified bentonite sample in order to monitor the change of the bentonite structure and crystallinity due to the modification process. The characterization was conducted using Rigaku Miniflex 600 equipped with Ni-filtered CuKα radiation at scanning speed 5° min^{-1}.

The surface functional group of natural bentonite and treated bentonite was evaluated using Fourier transform infrared (FTIR) spectroscopy. The samples were characterized using FTIR Shimadzu Prestige-21, and the spectrum was recorded at wavenumber 400 – 4000 cm^{-1} using KBr method.

Adsorption Experiment

All the adsorption process was systematically and totally conducted in batch adsorption method. Typically, a predetermined amount of adsorbent interacted with 50 mL of Cr (VI) solution in a conical flask at a constant temperature for a predetermined time. After finished, the remaining concentration of Cr (VI) solution was determined using UV-Vis spectrophotometer at wavelength 540 nm. The adsorption efficiency (%removal) and adsorption capacity (mg/g) at any time *t* (q_t) and equilibrium (q_e) were determined by the following equations:

$$\%\text{Removal} = \frac{C_0 - C_t}{C_0} x100 \tag{1}$$

$$q_t = \frac{(C_0 - C_t)V}{m} \tag{2}$$

$$q_e = \frac{(C_0 - C_e)V}{m} \tag{3}$$

Where C_o is the initial concentration of Cr (VI) solution (mg/L), C_t is the concentration of Cr (VI) after adsorbed at any time *t* (mg/L), and C_e is the concentration of Cr (VI) at equilibrium (mg/L). *V* is the volume of Cr (VI) solution (L), and *m* is the amount of adsorbent used (g).

Effect of some operational condition to the Cr (VI) adsorption efficiency was studied by varying the initial pH (3 – 8), adsorbent dosage (0.2 – 4 g/L), contact time (0 – 240 minutes), initial Cr (VI) concentration (1 – 10 mg/L), and temperature (30 – 60°C). Some adsorption parameters including adsorption kinetic, isotherm, and thermodynamic were also investigated based on the recent and most used models.

RESULTS AND DISCUSSION

In order to investigate the change of the bentonite, particularly the layer spacing, X-ray diffraction (XRD) analysis was subjected to NB, H-B and H-FePilB due to its high sensitivity to the change of crystallinity. The XRD diffraction pattern of NB, H-B, and H-FePilB was depicted in **FIGURE 1** and **TABLE 1.** As can be seen in the figure, the diffraction pattern of the natural bentonite exhibit seven characteristic diffraction pattern at 2θ of 6.39°, 19.77°. 22°, 26.6°, 28.6°, 34.9°, and 54°. The presence of the smectite phase in the natural bentonite was confirmed by the presence of the XRD pattern of montmorillonite, kaolinite, and quartz at 2θ value of 6.93°, 19.77°, and 26.6°, respectively [20]. The *d*(001) reflection of the bentonite ascribed to the ordering layer of the clay. For NB, *d*(001) reflection recorded at 2θ 6.39° with the basal spacing value 1.38 nm.

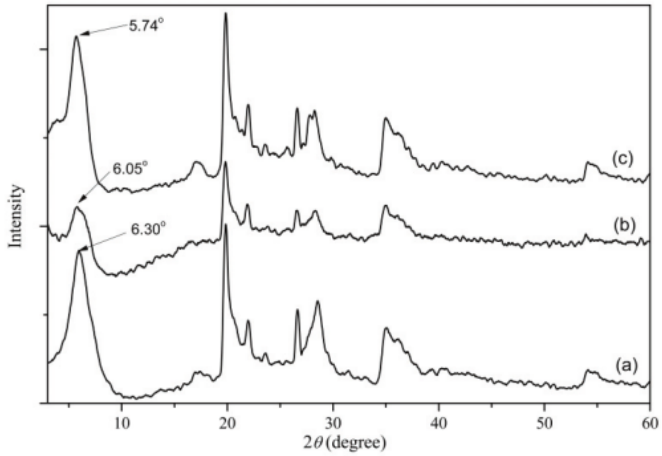

FIGURE 1. XRD pattern of bentonite (a), acid activated bentonite (b), and Fe-pillared acid activated bentonite (c)

The XRD pattern of the acid-treated bentonite exhibits slight differences compared with natural bentonite pattern, particularly at the *d*(001) characteristic peak. The reduction of the d001 peak intensity at 2θ around 6° indicates that the layer structure of the smectite was partially destructed. This finding also means that the crystallinity of the bentonite was affected during the acid activation process [20].

TABLE 1. XRD characteristic of natural and modified bentonite

Materials	2θ (deg)	d_{001} (nm)	Height (cps)	FWHM (deg)
N-Bent	6.39	1.382	712	1.53
H-Bent	6.05	1.459	457	5.10
H-FePilB	5.74	1.539	829	1.69

The XRD pattern of bentonite samples after acid-activated and iron pillared shows a significant incensement of the *d*(001) reflection peak and it was shifted toward lower degrees (**FIGURE 1**c). This finding indicates that the basal spacing of the smectite structure *d*(001) has enlarged due to the inclusion of hydroxyl-iron pillar into the interlayer space of the host bentonite. In another word, it means that the basal spacing value of the aluminosilicate layer increased. This incensement proofed that Fe-pillaring solution has successfully intercalated into bentonite interlayer space.

IR spectra of original bentonite (NB), H-B, and H-FePilB are presented in **FIGURE 2**. The spectra of natural and modified bentonite exhibit six characteristic absorption bands as described in **TABLE 2**. The presence of characteristic functional group of bentonite including Si-O stretching, Si-O-Al bending, and Si-O-Si bending vibration band was recorded at 1010 cm^{-1}, 516 cm^{-1}, and 478 cm^{-1}, respectively, for natural bentonite. IR spectra of acid treated bentonite exhibits significant changes compared with the natural bentonite spectra. Almost all the intensity of the characteristic bands reduced after acid treatment, particularly vibration band of Si-O stretching at 1010 cm^{-1}. This change indicates that the formation of slight amorphous structure of the silica due to the partial destruction in smectite structure. The spectra of iron pillared acid-activated bentonite exhibit notable changes compared with the spectra of acid activated bentonite spectra. The intensity of Si-O stretching band increased and shifted to the higher wavenumber that probably caused by the formation of protonic site due to the calcination of the intercalated cation [25].

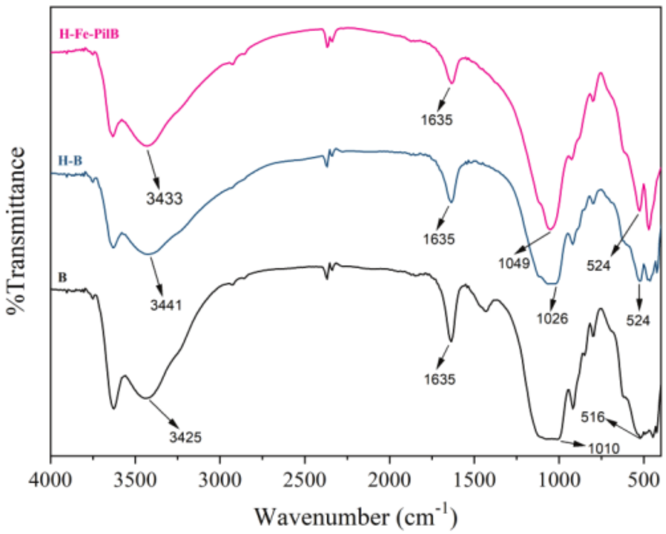

FIGURE 2. FT-IR spectra of bentonite (B), acid activated bentonite (H-B), and Fe-pillared acid activated bentonite (H-Fe-PilB)

TABLE 2. FTIR characteristic of natural and modified bentonite

Wavenumber (1/cm)			Functional group	References
NB	H-B	H-FePilB		
3626	3633	3633	Hydroxyl group assigned in octahedral structure	[23]
3441	3425	3433	Hydroxyl group assigned as water molecule in interlayer space	[26]
1635	1635	1635	O-H bending vibration	[27]
1010	1026	1049	Si-O stretching vibration	[28]
516	524	524	Si-O-Al bending vibration	[28]
478	462	470	Si-O-Si bending vibration	[28]

Adsorption Study

In adsorption system, the adsorbent dosage is one of the important parameters due to its effect on the adsorption capacity determination of an adsorbent in the system with constant concentration. Hence in this work, the effect of H-FePilB dosage on the adsorption efficiency of Cr (VI) was systematically conducted in various experiments with different adsorbent dosage used at constant Cr (VI) concentration. The results of this study are presented in **FIGURE 3**. As can be seen in the figure, the adsorption efficiency of Cr (VI) was gradually increased by increasing the adsorbent dosage from 0.2 to 2 g/L. However, when the adsorbent dosage was higher than 2 g/L the adsorption efficiency only slightly increased. In this case, by increasing the amount of the adsorbent in the adsorption system, the amount of the active site available to adsorb increased. Thus, the probability of Cr (VI) to be adsorbed on H-FePilB increased by increasing the amount of the adsorbent active site in the system [29].

The dependency of adsorption efficiency toward the contact time was an essential parameter to be studied. This investigation will give better understanding and information about the rate of the pollutant removal from the solution and also the time required for the adsorption process to achieve the equilibrium. These parameters are highly required for designing an efficient adsorption process.

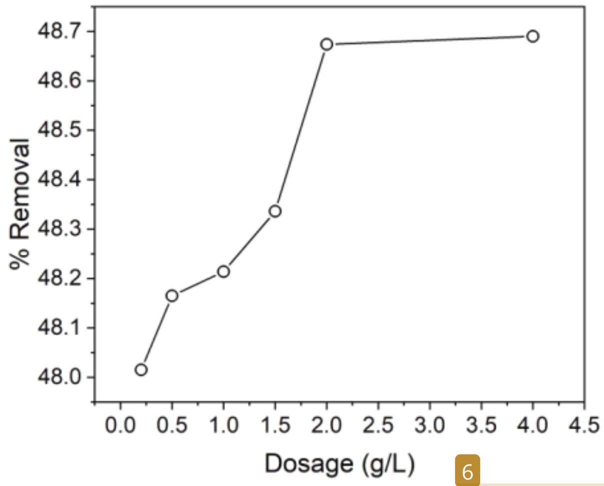

FIGURE 3. Effect of adsorbent dosage against the % removal of Cr(VI)

Study on the effect of contact time in Cr (VI) removal by H-FePilB was conducted in various contact time ranging from 0 to 240 minutes using constant adsorbent amount and Cr (VI) concentration. The results displayed in the form of absorbance and percent removal are presented in **FIGURE 4**. From the figure can be observed that Cr (VI) uptake on H-FePilB was occurred fast in the first 30 minutes and slightly increase over the time until the equilibrium was achieved. This finding indicates that in the early adsorption stage, the large number of the adsorption site in the H-FePilB was unoccupied. However, by increasing the contact time, the adsorption site was decreased and causing the reduction of the adsorption process [30].

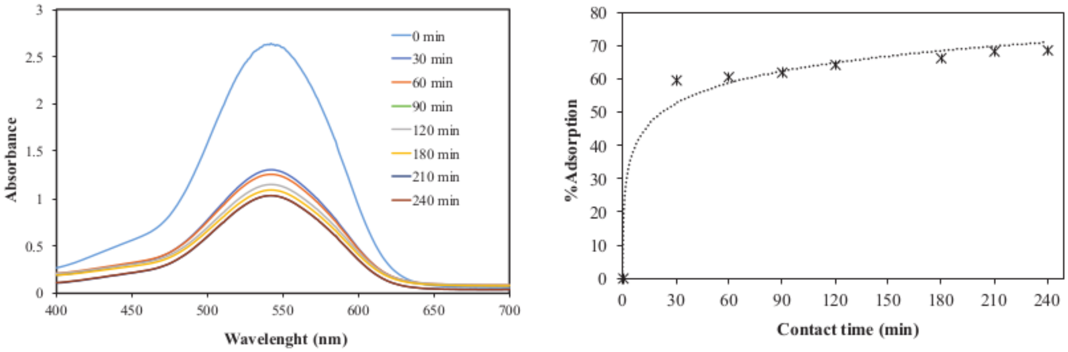

FIGURE 4. Effect of contact time against % adsorption of Cr(VI)

In order to investigate the mechanism of Cr (VI) adsorption on H-FePilB, the adsorption kinetics parameter was determined. The kinetics parameters for Cr (VI) adsorption was thoroughly investigated by interacting 5 mg/L of Cr (VI) solution with 0.05 g of H-FePilB for various contact time. The kinetics data obtained then formulated using two most studied kinetics models namely pseudo-first-order and pseudo-second-order.

The pseudo-first-order model was developed by Lagergren as presented in the following equation.

$$q_t = q_e(1 - e^{-k_1 t}) \qquad (4)$$

$$\log(q_e - q_t) = \log q_e - \frac{k_1}{2.303}t \qquad (5)$$

Where k_1 is the constant of pseudo-first-order rate (min^{-1}), q_t and q_e (mg/g) are the amounts of Cr (VI) adsorbed at any time t and equilibrium, respectively. The value of k_1 was determined from the slope value of $\log(q_e - q_t)$ against t.

The pseudo-second-order kinetics model was calculated based on the following equation:

$$q_t = k_2 \frac{q_e^2 t}{1 + k_2 q_e t} \qquad (6)$$

The arrangement of the equation (6) will give the linear form of the pseudo-second-order equation as follows:

$$\frac{t}{q_t} = \frac{1}{k_2 q_e^2} + \frac{t}{q_e} \qquad (7)$$

Where q_t is the amount of Cr (VI) adsorbed at time t (mg/g), qe is the amount of the Cr (VI) adsorbed at equilibrium (mg/g), and k_2 is constant related to the pseudo-second-order model (g/mg min). The initial concentration rate was determined using the following equation [31]:

$$k_0 = k_2 q_e^2 \qquad (8)$$

The fit of Cr (VI) adsorption data to the pseudo-first-order and pseudo-second-order model was illustrated in **FIGURE 5**, and its kinetics parameters obtained were tabulated in **TABLE 3**. As can be seen in **FIGURE 5**, the plot of pseudo-second-order model has better straight line compared with the pseudo-first-order model. The R^2 value for the pseudo-second-order model greater than 0.982 and the result of $q_{e,\,cal}$ value exhibits a little difference with $q_{e,\,exp}$. This finding confirmed that the kinetic adsorption of Cr (VI) was follow the pseudo-second-order model rather than the pseudo-first-order model [14].

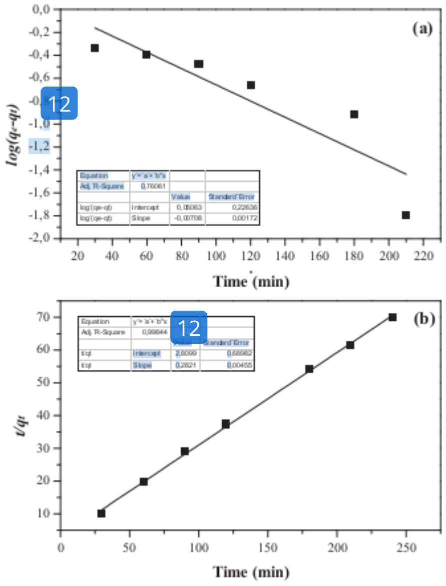

FIGURE 5. Pseudo-first-order (a), pseudo-second-order (b), fit model of Cr VI adsorption

TABLE 3. Kinetic parameter for Cr VI adsorption on H-FePilB

Pseudo-first-order	
$q_{e\ exp}$ (mg/g)	3.43
$q_{e\ cal}$ (mg/g)	1.12
k_1 (min^{-1})	0.0163
R^2	0.8085
Pseudo-second-order	
$q_{e\ cal}$ (mg/g)	3.54
$q_{e\ exp}$ (mg/g)	3.43
k_2 (g/mg min)	0.0283
h_o	0.3558
R^2	0.9987

CONCLUSION

Acid-activated followed by Fe-pillared of natural bentonite (H-FePilB) has been synthesized and characterized as an adsorbent for hexavalent chromium removal from aqueous solution. Cr (VI) removal was studied based on the effect of the operational parameter, adsorption kinetic, isotherm, and thermodynamic parameters. The optimum operational parameter for Cr (VI) removal by H-FePilB was at acidic solution condition, 2 g/L adsorbent dosage, 60 minutes contact time, and initial Cr (VI) concentration 5 mg/L. The kinetic adsorption was best fitted by pseudo-second-order model with qe value about 3.54 mg/g.

ACKNOWLEDGEMENT

Profoundly, TT thanks to the Ministry of Research, Technology, and Higher Education of Republic Indonesia, for financially supporting this research through "*Program Magister Menuju Doktor untuk SarjanaUnggul*" (PMDSU) grant with contract number 468/UN9.3/LT/2017 and 326/SP2H/LT/DRPM/IX/2016.

REFERENCES

1. M.H. Dehghani, D. Sanaei, I. Ali, and A. Bhatnagar, J. Mol. Liq. **215**, 671–679 (2016).
2. G. Wang, Y. Hua, X. Su, S. Komarneni, S. Ma, and Y. Wang, Appl. Clay Sci. **124–125**, 111–118 (2016).
3. A. Kumar and H.M. Jena, Process Saf. Environ. Prot. **109**, 63–71 (2017).
4. J. Qian, J. Zhou, L. Wang, L. Wei, Q. Li, D. Wang, and Q. Wang, Chem. Eng. J. **309**, 330–338 (2017).
5. C.-C. Wang, X.-D. Du, J. Li, X.-X. Guo, P. Wang, and J. Zhang, Appl. Catal. B Environ. **193**, 198–216 (2016).
6. L.-L. Li, X.-Q. Feng, R.-P. Han, S.-Q. Zang, and G. Yang, J. Hazard. Mater. **321**, 622–628 (2017).
7. E. Abbasi-Garravand and C.N. Mulligan, Sep. Purif. Technol. **132**, 505–512 (2014).
8. L. Li, Y. Li, and C. Yang, Carbohydr. Polym. **140**, 299–307 (2016).
9. W. Jin, H. Du, S. Zheng, and Y. Zhang, Electrochim. Acta **191**, 1044–1055 (2016).
10. T. Taher, R. Mohadi, and A. Lesbani, Rasayan J. Chem. **11**, 1244–1254 (2018).
11. Q. Xu, Y. Wang, L. Jin, Y. Wang, and M. Qin, J. Hazard. Mater. **339**, 91–99 (2017).
12. S.A. Chaudhry, T.A. Khan, and I. Ali, J. Mol. Liq. **236**, 320–330 (2017).
13. C.-Y. Cao, C.-H. Liang, Y. Yin, and L.-Y. Du, Mar. Georesources Geotechnol. **34**, 764–769 (2016).
14. K.M. Doke and E.M. Khan, Arab. J. Chem. **10**, S252–S260 (2017).
15. P. Miretzky and A.F. Cirelli, J. Hazard. Mater. **180**, 1–19 (2010).
16. A. León-Torres, E.M. Cuerda-Correa, C. Fernández-González, M.F. Alexandre Franco, and V. Gómez-Serrano, J. Colloid Interface Sci. **386**, 325–332 (2012).
17. B.R. Araújo, J.O.M. Reis, E.I.P. Rezende, A.S. Mangrich, A. Wisniewski, D.P. Dick, and L.P.C. Romão, J. Environ. Manage. **129**, 216–223 (2013).
18. R. Upadhyay, P.K. Pandey, and Pardeep, Mater. Today Proc. **4**, 10504–10508 (2017).
19. A.A. Bakr, N.A. Sayed, T.M. Salama, I.O. Ali, R.R.A. Gayed, and N.A. Negm, Res. Chem. Intermed. **44**, 389–405 (2018).
20. R.R. Pawar, H.C. Bajaj, and S. Lee, J. Ind. Eng. Chem. **34**, 213–223 (2016).

21. E. Orucoglu and S. Haciyakupoglu, J. Environ. Manage. **160**, 30–38 (2015).
22. L.G. Yan, Y.Y. Xu, H.Q. Yu, X.D. Xin, Q. Wei, and B. Du, J. Hazard. Mater. **179**, 244–250 (2010).
23. H. Faghihian and M.H. Mohammadi, Appl. Surf. Sci. **264**, 492–499 (2013).
24. C. Cao, L. Meng, and Y. Zhao, Toxicol. Environ. Chem. **2248**, 37–41 (2013).
25. P. Kumararaja, K.M. Manjaiah, S.C. Datta, and B. Sarkar, Appl. Clay Sci. **137**, 115–122 (2017).
26. A.A. Atia, Appl. Clay Sci. **41**, 73–84 (2008).
27. V.K. Gupta, M. Sharma, and R.K. Vyas, J. Environ. Chem. Eng. **3**, 2172–2179 (2015).
28. J. Nones, J. Nones, A. Poli, A.G. Trentin, H.G. Riella, and N.C. Kuhnen, Colloids Surfaces B Biointerfaces **145**, 555–561 (2016).
29. R. Huang, B. Wang, B. Yang, D. Zheng, and Z. Zhang, Desalination **280**, 297–304 (2011).
30. S. Du, L. Wang, N. Xue, M. Pei, W. Sui, and W. Guo, J. Solid State Chem. **252**, 152–157 (2017).
31. H. Koyuncu, Appl. Clay Sci. **38**, 279–287 (2008).

C.2a.1.11-Adsorption behavior of Cr (VI) from aqueous.pdf

ORIGINALITY REPORT

21%

SIMILARITY INDEX

PRIMARY SOURCES

1	rasayanjournal.co.in Internet	125 words — 3%
2	aip.scitation.org Internet	110 words — 3%
3	www.researchgate.net Internet	98 words — 3%
4	mafiadoc.com Internet	93 words — 3%
5	link.springer.com Internet	58 words — 2%
6	ujcontent.uj.ac.za Internet	58 words — 2%
7	journals.plos.org Internet	47 words — 1%
8	media.neliti.com Internet	38 words — 1%
9	repository.unkhair.ac.id Internet	27 words — 1%
10	budi.ristekdikti.go.id Internet	

24 words — 1%

11 iopscience.iop.org
Internet
24 words — 1%

12 repositorio.unifei.edu.br
Internet
24 words — 1%

13 www.hindawi.com
Internet
18 words — 1%

EXCLUDE QUOTES	OFF	EXCLUDE MATCHES	< 1%
EXCLUDE BIBLIOGRAPHY	ON		